

A NEW RADIO – X-RAY PROBE OF GALAXY CLUSTER MAGNETIC FIELDS

T. E. CLARKE¹

Department of Astronomy, University of Toronto, 60 St. George St., Toronto, ON M5S 3H8 Canada

P. P. KRONBERG

Department of Physics, University of Toronto, 60 St. George St., Toronto, ON M5S 1A7 Canada

AND

HANS BÖHRINGER

Max-Planck-Institut für extraterrestrische Physik, D-85740 Garching, Germany

Draft version November 16, 2018

ABSTRACT

Results are presented of a new VLA–ROSAT study that probes the magnetic field strength and distribution over a sample of 16 “normal” low redshift ($z \leq 0.1$) galaxy clusters. The clusters span two orders of magnitude in X-ray luminosity, and were selected to be free of (unusual) strong radio cluster halos, and widespread cooling flows. Consistent with these criteria, most clusters show a relaxed X-ray morphology and little or no evidence for recent merger activity.

Analysis of the rotation measure (RM) data shows cluster-generated Faraday RM excess out to $\sim 0.5 h_{75}^{-1}$ Mpc from cluster centers. The results, combined with RM imaging of cluster-embedded sources and ROSAT X-ray profiles indicates that the hot intergalactic gas within these “normal” clusters is permeated with a high filling factor by magnetic fields at levels of $\langle |B| \rangle_{icm} = 5\text{--}10$ $(\ell/10 \text{ kpc})^{-1/2} h_{75}^{1/2} \mu\text{G}$, where ℓ is the field correlation length. These results lead to a global estimate of the total magnetic energy in clusters, and give new insight into the ultimate energy origin, which is likely gravitational. These results also shed some light on the cluster evolutionary conditions that existed at the onset of cooling flows.

Subject headings: galaxies: clusters: general — magnetic fields — polarization — radio continuum: galaxies — X-rays: general

1. INTRODUCTION

Determinations of magnetic field strengths in the intracluster medium over the past decade have revealed fields of unanticipated strength in some clusters. Additionally, these studies have raised apparent contradictions between field strengths (or limits) obtained from different observational methods. In order to understand the physical conditions in the intracluster medium, it is important to understand the origin(s) of cluster fields, and the astrophysical processes that relate them to other energy constituents of the cluster gas.

Estimates of magnetic field strengths in the intracluster medium (ICM) can be determined from measurements of Faraday rotation through the intracluster gas, and an independent measurement of the ICM thermal electron density, n_e . Faraday rotation is given by:

$$\text{RM} = \frac{\Delta\chi}{\Delta\lambda^2} = 811.9 \int_0^L n_e B_{\parallel} dl \text{ rad m}^{-2}, \quad (1)$$

where χ is the position angle of the linearly polarized radiation at wavelength λ , n_e is the thermal electron density in cm^{-3} , B_{\parallel} is the line of sight magnetic field strength in μG , and L is the path length in kpc. The thermal electron density in a cluster can be determined from X-ray surface brightness profiles of the hot ($T \sim 10^8$ K), diffuse ($n_e \sim 10^{-3} h_{75}^{1/2} \text{cm}^{-3}$) gas (Böhringer 1995) which fills the cluster potential.

The first study of background RMs over a *single* clus-

ter (Kim et al. 1990) was a targeted set of deep VLA observations of 18 sources close in angular position to the Coma cluster (which has no cooling flow, but a strong synchrotron halo). The result of the study was $\langle |B| \rangle_{icm} = 2.5 (\ell/10 \text{ kpc})^{-1/2} h_{75}^{1/2} \mu\text{G}$ where ℓ is the B-reversal scale. In a subsequent study by Feretti et al. (1995) the discovery of smaller ℓ scales down to 1 kpc raised this estimate to $\sim 7.2 h_{75}^{1/2} \mu\text{G}$ for Coma.

Studies of a large number of galaxy clusters with many RM probes per cluster are currently unfeasible given the sensitivity limits of available radio telescopes, combined with the small angular size of more distant clusters. This situation can be circumvented by obtaining RM probes through a sample of clusters, each having typically only one or two (bright) polarized radio sources. The consensus of these studies (Lawler & Dennison 1982; Kim et al. 1991; Goldshmidt & Rephaeli 1993) is that cluster cores have a detectable component of RM, and many have field strengths at the microgauss level. Note that the Faraday study by Hennessy, Owen, & Eilek (1989) does not find evidence for intracluster magnetic fields. This discrepancy is, however, likely due to the combination of small statistics and large impact parameters in their study.

For a few clusters with extensive cooling flows, high resolution Faraday rotation measure mapping of extended sources that are embedded within the cooling flow zones have, in combination with X-ray data, produced magnetic

¹present address: NRAO, 1003 Lopezville Rd., Socorro, N.M. 87801 USA

field strength estimates of 10–40 μG , ordered on scales varying from 100 – 0.5 kpc (see Taylor, Allen, & Fabian 1999, and references therein).

Lower limits to ICM magnetic field strengths in the range 0.1 – 1 μG level have been suggested from recent detections of both excess (over thermal) extreme ultraviolet (EUV) and hard X-ray (HEX) emission in some clusters. These field values would seem to *prima facie* contradict the much higher values above *if* the EUV excess emission is interpreted as inverse Compton (IC) scattering of ~ 100 MeV electrons (Rephaeli, Ulmer, & Gruber 1994). The EUV detections (Bowyer, Berghöfer, & Korpela 1999) in particular apply to only a few clusters having widespread extended synchrotron emission and/or they occur near to the cooling flow zone (as in M87). Spatial differentiation of high and low magnetic field regions in the ICM avoids the apparent contradiction by allowing the synchrotron and EUV IC emission to originate in low field regions, while high field regions, where the synchrotron energy loss time is short, would provide the major contribution to the Faraday rotation measures (Enßlin, Lieu, & Biermann 1999). Further, EUV emission also appears not to be cluster wide, but concentrated to central sub-regions, and hence does not spatially correspond to the wider regions probed by the X-ray emission and Faraday RM measurements. The HEX excess in clusters can be plausibly understood as bremsstrahlung from a (probably shock heated) population of suprathermal electrons (Enßlin, Lieu, & Biermann 1999; Dogiel 1999; Sarazin & Kempner 2000). Thus, on balance, it appears that spatial differentiation of field regions and/or emission mechanisms other than IC scattering of CMB photons are more plausible where apparent contradictions in magnetic field estimates arise.

This paper concentrates on what we shall term “normal” Abell clusters *i.e.* those which have neither *widespread* cooling flows nor strong synchrotron halos. The observations are aimed at estimating the strength and spatial extent of intracluster medium magnetic fields for a relatively homogeneous sample of 16 Abell clusters. Throughout this *Letter*, we adopt $H_0 = 75 h_{75} \text{ km s}^{-1} \text{ Mpc}^{-1}$, and $q_0=0.5$.

2. SELECTION OF THE CLUSTERS

Each target cluster in our sample was required to have bright ($L_x > 5 \times 10^{42} h_{75}^{-2} \text{ ergs s}^{-1}$), extended X-ray emission in ROSAT observations. Therefore, the majority of the target galaxy clusters in our sample fall within the low redshift ($z \leq 0.1$) part of the X-ray-brightest Abell-type clusters of galaxies (XBACs, Ebeling et al. 1996) sample. The XBACs clusters are limited to high Galactic latitudes ($|\text{b}| \geq 20^\circ$), low redshifts ($z \leq 0.2$), and ROSAT 0.1–2.4 keV band X-ray fluxes above $5.0 \times 10^{-12} \text{ ergs cm}^{-2} \text{ s}^{-1}$. A further selection constraint was that each cluster was required to have at least one linearly polarized radio source viewed through the X-ray emitting gas. Such radio sources are referred to as the *cluster* sample. A second set of polarized (*control*) radio sources viewed, in projection, outside the boundary of the X-ray emission was also selected for each target galaxy cluster. All polarized radio targets

(*cluster* and *control*) were selected from the NRAO VLA Sky Survey (NVSS, Condon et al. 1998) data.

Galaxy cluster selection was further constrained such that the sightlines of the target radio sources probed, collectively, the largest possible range of impact parameters. The sources also had to have sufficient polarized flux density that follow-up polarimetry could be undertaken in short integrations (~ 5 minutes) at the VLA². Specifically the inclusion criterion required $I_{1.4} > 100 \text{ mJy}$ and 1.4 GHz polarization, $m_{1.4}$, greater than 1% in the NVSS survey. A complete description of the galaxy cluster and radio source samples will be presented in Clarke, Kronberg, & Böhringer (in preparation).

The final sample consists of 16 Abell clusters, 13 of which are members of the XBACs sample. The three non-XBACs clusters fall slightly below the flux limit for inclusion in the XBACs sample. Our 16 cluster sample was reduced from an original 24 that fell within the above criterion as severe radio frequency interference, which is endemic to some of the crucial (for RM) 20 cm bands, reduced the reliability of some RMs. To optimize data quality, we reduced the final sample to 16, since even this smaller number was statistically adequate.

It is important to mention *ab initio* two types of systematic bias that might result from the above selection criteria. First, the condition $m_{1.4} > 1\%$ may preferentially select against regions of very high Faraday rotation, whose signature would be low polarization at the longer radio wavelengths. This could have caused some high RMs, but not low RMs, to have been missed in our cluster sample. This would statistically understate the clusters’ true rotation measure distribution, and hence magnetic field strengths. Second, the very innermost regions of the cluster cores, which in some cases may have a cooling flow, will have been missed because of their small angular cross sections. We do not consider this second form of bias to be serious, since this investigation is targeted to cluster volumes that do *not* have strong cooling flows.

3. OBSERVATIONS AND ANALYSIS OF THE DATA

3.1. Radio

Target radio sources selected from the NVSS survey were re-observed with the VLA at four to six wavelengths within the 20 cm and 6 cm bands. These wavelengths were selected to provide Faraday rotation measures that are unambiguous within the range $|\text{RM}| \leq 2600 \text{ rad m}^{-2}$. The observations were undertaken in October and December 1995, August 1996, and September 1997 in the VLA’s B, D, and CS configurations respectively.

The radio data were reduced within the NRAO AIPS package following the standard Fourier transform, deconvolve, and restore method. In addition, self-calibration was applied to each source to further reduce the effects of phase fluctuations. Images in the Stokes I, Q, and U parameters were produced for each source at each of at least four wavelengths.

3.2. X-ray

²The National Radio Astronomy Observatory is a facility of the National Science Foundation operated under cooperative agreement by Associated Universities, Inc

³The ROSAT Data Archive is maintained by the Max-Planck-Institut für extraterrestrische Physik (MPE) at Garching, Germany.

X-ray observations of each galaxy cluster were retrieved from the ROSAT Data Archive³. Thirteen of the target clusters were in the Pointed Observation archive while the data for the remaining three clusters were extracted from the ROSAT All-Sky Survey archive. All extracted X-ray data were taken using one of ROSAT’s Position Sensitive Proportional Counters (PSPCs) which have moderate angular resolution (FWHM $\sim 25''$) and are sensitive to photons in range of 0.1 – 2.4 keV.

The ROSAT X-ray data were reduced using the Extended X-ray Scientific Analysis Software (EXSAS, Zimmermann et al. 1994) package under the European Southern Observatory’s (ESO’s) Munich Image Data Analysis System (MIDAS). A radial X-ray surface brightness profile was determined for each cluster by integrating the PSPC photon events over concentric annuli of $15''$ and $30''$ for the ROSAT Pointed and RASS Observations respectively. The surface brightness profiles were fit with a hydrostatic isothermal model (Sarazin 1986).

4. RESULTS

The observed Faraday rotation measure of an individual source is an algebraic sum of Faraday contributions due to our Galaxy, the cluster, any source-intrinsic component, and the general IGM. The latter three are usually small, and the Galactic RM contribution was statistically removed by subtracting the mean RM over all non-cluster sources within 10° of the cluster center from that of the radio probe in question. Due to the high Galactic latitudes of the target clusters, the mean Galactic contribution in the present sample is fairly small, on average 9.5 rad m^{-2} . The cluster radio sources and associated Galaxy-corrected RMs are listed in Table 1.

In Figure 1 we plot the residual rotation measure of the radio sources as a function of cluster impact parameter in kiloparsecs. This figure displays a clear Faraday excess in radio sources viewed through the X-ray emitting ICM (open points) as compared to those viewed beyond the detectable edge of the thermal cluster gas. The RM distribution of the *control* sources has a width of 15 rad m^{-2} while that of the *cluster* sources viewed through the ICM is much broader at 114 rad m^{-2} . The Kolmogorov-Smirnov test rejects the null hypothesis that the two samples were drawn from the same population with a confidence level of 99.5%. This confirms the detection of an intracluster Faraday rotating medium.

Determination of magnetic field strengths at various impact parameters within our cluster sample requires some assumption about the field topology along the line of sight to the radio probe. The simplest model of the ICM magnetic fields is a “uniform slab” in which the magnetic field has constant strength and direction through the entire cluster. Using this model and the X-ray determined electron densities, Equation 1 yields magnetic field strengths between $\sim 0.5 - 3.0 h_{75}^{1/2} \mu\text{G}$ across the Faraday sample. More realistically, there are reversals along the line of sight to the radio source probe. In the simple case of an intracluster medium composed of \mathcal{N} cells of uniform size and field strength, but random field directions, the field in an individual cell increases as $\sqrt{\mathcal{N}}$ over the uniform slab estimate. Using a simple tangled cell model with a constant coherence length, $\ell = 10 h_{75}^{-1} \text{ kpc}$, yields an

average intracluster magnetic field strength estimate of $\sim 5(\ell/10 \text{ kpc})^{-1/2} h_{75}^{1/2} \mu\text{G}$. This coherence length ℓ , estimated from RM images of three extended radio sources in our sample (see below), is limited by the resolution of our images. Because $\langle \ell(r) \rangle$ may systematically change (*e.g.* increase with r) this “global” average field value could increase to values as high as $10 h_{75}^{1/2} \mu\text{G}$ near the cluster cores.

The distribution of excess RM’s appears to cutoff close to the observed X-ray outer boundary. This result, though interesting and new, requires more detailed X-ray and radio data to understand the variation of the magnetic to thermal energy density $\varepsilon_B(r)/\varepsilon_{th}(r)$ throughout the ICM.

A striking effect, seen in Figure 1, is the virtual exclusion of small RMs at $r \leq 500 h_{75}^{-1} \text{ kpc}$. This suggests that the RM filling factor in normal galaxy clusters is very high. An independent, quantitative estimate of the RM filling factor is provided from analysis of multi-frequency polarization images of three extended radio sources, 0039+212, 0056-013, and 1650+815 (J2000) that are embedded within three of our clusters (Abell 75, 119, and 2247 respectively). These sources project a combined area of $2.5 \times 10^4 \text{ kpc}^2$, and consist of 3 sets of 30, 48, and 24 contiguous independent RM sightlines, each of which has approximately the same areal cross-section: $\sim (5 \text{ kpc})^2$. The individual RM histograms across the three sources are consistent with normal distributions with means of -60, -144, and -97 rad m^{-2} . We find that 95% of the sightlines within this subset of three clusters have RMs significantly higher than the dispersion for non-cluster sightlines, $|\text{RM}| = 15 \text{ rad m}^{-2}$. This implies that the areal filling factor of magnetic fields is *at least* 95% in the ICM. This strongly suggests that these enhanced magnetic field levels permeate the clusters with a high filling factor, since within cell sizes down to a resolution of 10 kpc almost no ray passing through the ICM escapes some magnetized region.

5. DISCUSSION

These results confirm the widespread existence of magnetic fields in the central regions of non cooling flow clusters. The cluster-enhanced RM can generally be traced out to the periphery of the ROSAT-detectable ICM X-ray emission. The rotation measure distribution across our cluster sample drops from $\sim 200 \text{ rad m}^{-2}$ in the central regions (which may be an underestimate, see §2) to the background level of $\sim 15 \text{ rad m}^{-2}$ at large radii.

Our new measurements of (1) the RM, (2) the intracluster electron density, (3) the magnetic field volume filling factor, and (4) the average tangling scale of the field enable us to estimate, even if only crudely, an important physical quantity – the total energy in the ICM magnetic field for “normal”, non-merging, relaxed clusters. For a $5 h_{75}^{1/2} \mu\text{G}$ magnetic field in the inner $500 h_{75}^{-1} \text{ kpc}$ sphere, the total magnetic energy is $E_B = 1.5 \times 10^{61} (\frac{r}{500 \text{ kpc}})^3 (\frac{B}{5 \mu\text{G}})^2 h_{75}^{-2} \text{ ergs}$. The magnetic energy content of the ICM can then be compared to the total thermal energy content in the same cluster volume. The latter is (again taking constant values within a fiducial radius that is close to both the RM cutoff radius in Figure 1 and the X-ray radius) $E_{th} =$

$6.4 \times 10^{62} n_e \left(\frac{r}{500 \text{ kpc}} \right)^3 \left(\frac{T}{10^8 \text{ K}} \right) h_{75}^{-2}$ ergs, where n_e is the intracluster electron density in units of $10^{-3} h_{75}^{1/2} \text{ cm}^{-3}$. The ratio $\frac{E_B}{E_{th}}$ is of order 2.5%, and the possibility that $|B|$ may be underestimated due to limited radio resolution makes it possible that $\frac{E_B}{E_{th}}$ could be even higher. Even at the lower bound of 2.5% the ratio suggests that the magnetic energy provides a non-negligible fraction of the energy budget of the ICM.

We can now compare this approximate magnetic energy estimate with other sources of energy that are relevant for a cluster: the thermonuclear (stellar) energy released in all cluster-member galaxies, the gravitational binding energy released from AGN/accretion disks, the cluster gas binding energy, and the energy associated with past merger events. The available energy from stellar sources cannot be much greater than $\sim 10^{62}$ ergs (Völk & Atoyan 2000), *i.e.* of comparable magnitude, and is thus insufficient to maintain the magnetic fields, barring a very high energy conversion efficiency. This means that thermonuclear energy can be ruled out as the primary source of intracluster magnetic field energy. It must therefore be ultimately derived from gravity. A single powerful AGN/accretion disk can be expected to inject approximately 10^{61} ergs over its lifetime into the ICM. Comparing the lifetime of the radio source with the cluster lifetime we expect 10^2 sources to have injected a total of $\sim 10^{62} - 10^{63}$ ergs into the

ICM. This makes AGN/accretion disks an attractive possible source of the ICM field energy, as has been suggested by Colgate & Li (1999). Other sources of ICM magnetic energy are the gravitational binding energy of the cluster gas, which is of order 10^{64} ergs, and the energy associated with a past cluster merger event, which is of order 10^{63-64} ergs. This suggests that the magnetic energy possibly “taps into” a combination of the gravitational energy released in AGN/accretion disks over the lifetimes of clusters, and shearing and shocks associated with larger scale infall of matter as the clusters evolve.

Given that the cooling flows represent a late stage of cluster evolution and our “global” value of $5 h_{75}^{1/2} \mu\text{G}$ for ICM zones within the clusters, but outside of cooling flow zones, we conclude that the cooling flow develops out of a medium whose field strength is already a significant fraction of what is seen in the cooling flow zones.

P.P.K. acknowledges the support of the Natural Sciences and Engineering Research Council of Canada (NSERC) and the support of a Killam Fellowship, and T.E.C. is grateful for the support of NSERC, OGS, and I.O.D.E. scholarships, and the Sumner Fellowship. We acknowledge beneficial discussions with Stirling Colgate, Jean Eilek, Torsten Enßlin, Jim Felten, and Greg Taylor, and we thank the referee for helpful comments.

REFERENCES

- Böhringer, H. 1995, *Rev. Mod. Astron.*, 8, 295
 Bowyer, S., Berghöfer, T.W. & Korpela, E. 1999, in *Diffuse Thermal and Relativistic Plasma in Galaxy Clusters*, eds. H. Böhringer, L. Feretti, & P. Schuecker, MPE Report 271, 201
 Colgate, S.A. & Li, H. 1999, in *Highly Energetic Physical Processes, and Mechanisms for Emission from Astrophysical Plasmas*, eds. P.C.H. Martens & S. Tsuruta. ASP Conf. Series 334, 255
 Condon, J.J., Cotton, W.D., Greisen, E.W., Yin, Q.F., Perley, R.A., Taylor, G.B., & Broderick, J.J. 1998, *AJ*, 115, 1693
 Dogiel, V.A. 1999, in *Diffuse Thermal and Relativistic Plasma in Galaxy Clusters*, eds. H. Böhringer, L. Feretti, & P. Schuecker, MPE Report 271, 259
 Ebeling, H., Voges, W., Böhringer, H., Edge, A.C., Huchra, J.P., & Briel, U.G. 1996, *MNRAS*, 281, 799
 Enßlin, T.A., Lieu, R. & Biermann, P.L. 1999, *A&A*, 344, 409
 Feretti, L., Dallacasa, D., Giovannini, G., & Tagliani, A. 1995, *A&A*, 302, 680
 Goldshmidt, O. & Rephaeli, Y. 1993, *ApJ*, 411, 518
 Hennessy, G.S., Owen, F.N., & Eilek, J.A. 1989, *ApJ*, 347, 144
 Kim, K.-T., Kronberg, P.P., Dewdney, P.D., & Landecker, T.L. 1990, *ApJ*, 355, 29
 Kim, K.-T., Tribble, P.C., & Kronberg, P.P. 1991, *ApJ*, 379, 80
 Lawler, J.M. & Dennison, B. 1982, *ApJ*, 252, 81
 Rephaeli, Y., Ulmer, M., & Gruber, D. 1994, *ApJ*, 429, 554
 Sarazin, C.L. 1986, *Rev. Mod. Phys.*, 58, 1
 Sarazin, C.L., & Kempner, J.C. 2000, *ApJ*, 533, 73
 Taylor, G.B., Allen, S.W., & Fabian, A.C. 1999, in *Diffuse Thermal and Relativistic Plasma in Galaxy Clusters*, eds. H. Böhringer, L. Feretti, & P. Schuecker, MPE Report 271, 77
 Völk, H.J. & Atoyan, A.M. 2000, *ApJ*, 541, 88
 Zimmermann, H.U., Becker, W., Belloni, T., Döbereiner, S., Izzo, C., Kahabka, P., & Schwentker, O. 1994, *EXSAS User's Guide*, MPE Report 244

TABLE 1
CLUSTER SAMPLE RADIO SOURCES

Source (J2000)	Abell	L_x^a (10^{44} ergs s^{-1})	b^b (kpc)	RM ^c	\pm RM
0039+212	75	0.26	100	-62.62	9.03
0040+212	75	0.26	480	-34.00	10.95
0042-092	85	3.96	960	4.88	9.77
0056-013	119	1.55	280	-149.16	10.68
0057-013	119	1.55	1020	14.02	10.17
0126-013a	194	0.06	140	94.22	12.25
0154+364	262	0.28	570	-202.36	4.31
0245+368	376	0.57	630	-48.06	5.92
0257+130	399	2.60	280	-185.89	6.47
0318+419	426	6.36	550	6.17	15.40
0316+412	426	6.36	740	74.94	9.26
0434-131	496	1.52	310	52.91	6.69
0434-133	496	1.52	360	35.89	6.73
0709+486	569	0.02	3	-229.74	7.75
0909-093	754	3.98	1010	-20.47	9.16
0908-100	754	3.98	1460	12.35	9.43
0919+334	779	0.07	560	16.55	8.38
1037-270	1060	0.23	410	9.38	6.18
1037-281	1060	0.23	510	25.21	8.19
1039-273	1060	0.23	530	103.99	6.33
1039-272	1060	0.23	620	103.73	11.51
1036-267	1060	0.23	640	25.76	16.23
1133+489a	1314	0.20	270	68.05	6.42
1133+490	1314	0.20	310	-50.38	6.40
1145+196	1367	0.68	170	257.46	11.73
1650+815a	2247	0.06	200	-127.36	8.56
1650+815b	2247	0.06	270	-131.75	8.56

^aX-ray luminosity in the ROSAT 0.1 – 2.4 keV band determined from the current work.

^bCluster-centric impact parameter of radio source.

^cGalaxy-corrected rotation measure.

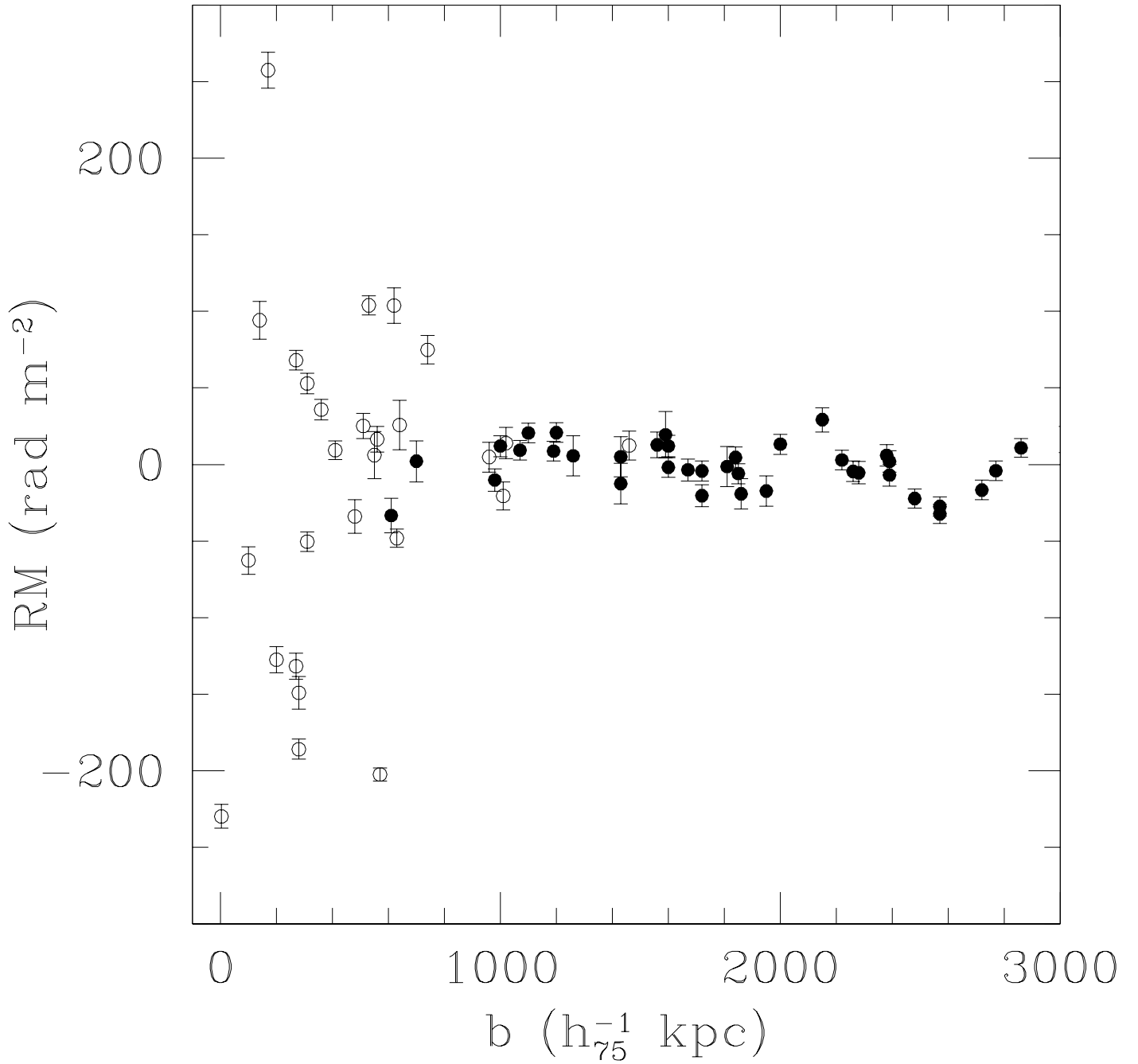


FIG. 1.— Galaxy-corrected rotation measure plotted as a function of source impact parameter in kiloparsecs for the sample of 16 Abell clusters. The open points represent the *cluster* sources viewed through the thermal cluster gas while the closed points are the *control* sources at impact parameters beyond the cluster gas. Note the clear increase in the width of the RM distribution toward smaller impact parameter.